Available online at www.sciencedirect.com
SCIENCE DIRECT®
Marine Geology 201 (2003) 287–305
MARINE GEOLOGY
INTERNATIONAL JOURNAL OF MARINE GEOLOGY, GEOCHEMISTRY AND GEOPHYSICS
www.elsevier.com/locate/margeo

Bottom current-controlled sedimentation and mass wasting in the northwestern Sea of Okhotsk

H.K. Wong[a,*], T. Lüdmann[a], B.V. Baranov[b], B.Ya. Karp[c], P. Konerding[a], G. Ion[d]

[a] Institute of Biogeochemistry and Marine Chemistry, Hamburg University, Bundesstraße 55, 20146 Hamburg, Germany
[b] P.P. Shirshov Institute of Oceanology, Russian Academy of Sciences, 36 Nakhimovkii Prospect, 117218 Moscow, Russia
[c] Pacific Oceanology Institute, Far Eastern Branch of the Russian Academy of Sciences, 43 Baltiskaya, 6690041 Vladivostok, Russia
[d] National Institute of Marine Geology and Geoecology, 23–25 Dimitrie Onciul Street, 70138 Bucharest, Romania

Received 17 May 2002; accepted 24 June 2003

Abstract

Quaternary sedimentation in the northwestern Sea of Okhotsk, where tidal and thermohaline currents are active, was studied using 8443 km of high-resolution air gun profiles from four cruises. It is characterized by: (1) bottom current-controlled processes, which lead to widespread deposition of contourite drifts and sediment waves on the North Okhotsk continental margin and the northernmost Sakhalin slope, as well as to erosion and sediment reworking on the northern Sakhalin shelf; (2) mass wasting triggered probably by shallow earthquakes, by gas hydrate instability during sea-level lowstands leading to slumps and debris flows in the western Derugin Basin; (3) deposition of the fluvial load of the River Amur, which results in sediment drift bodies and prograding lowstand wedges during glacial periods, and to contourite drifts and a 'fan' during interglacial times; and (4) ice-rafted detritus and hemipelagic sedimentation interrupted by episodic turbidity current activity, especially in the Derugin Basin and its northern, eastern and southern flanks.

Keywords: Sea of Okhotsk; contourite drifts; sediment waves; mass wasting

1. Introduction

The Sea of Okhotsk is a large, as yet poorly studied marginal sea at the northwestern rim of the Pacific. Its northwestern part consists of the northern Sakhalin margin, the western North Okhotsk margin (including Staretsky Trough and Kashevarov Bank) as well as the Derugin Basin (Fig. 1). The continental shelf of the northern Sakhalin margin averages 60–90 km in width, the maximum being 140 km off the northern tip of Sakhalin Island. Staretsky Trough, with water depths of 500–1000 m, strikes NW–SE and separates the Sakhalin slope from the Kashevarov Bank. This bank is formed by basement uplift. It is 50 × 200 km in dimension and has a steep southwestern flank. The top of Kashevarov

* Corresponding author.
E-mail address: hkwong@geowiss.uni-hamburg.de (H.K. Wong).

0025-3227/03/$ – see front matter © 2003 Elsevier B.V. All rights reserved.
doi:10.1016/S0025-3227(03)00221-4

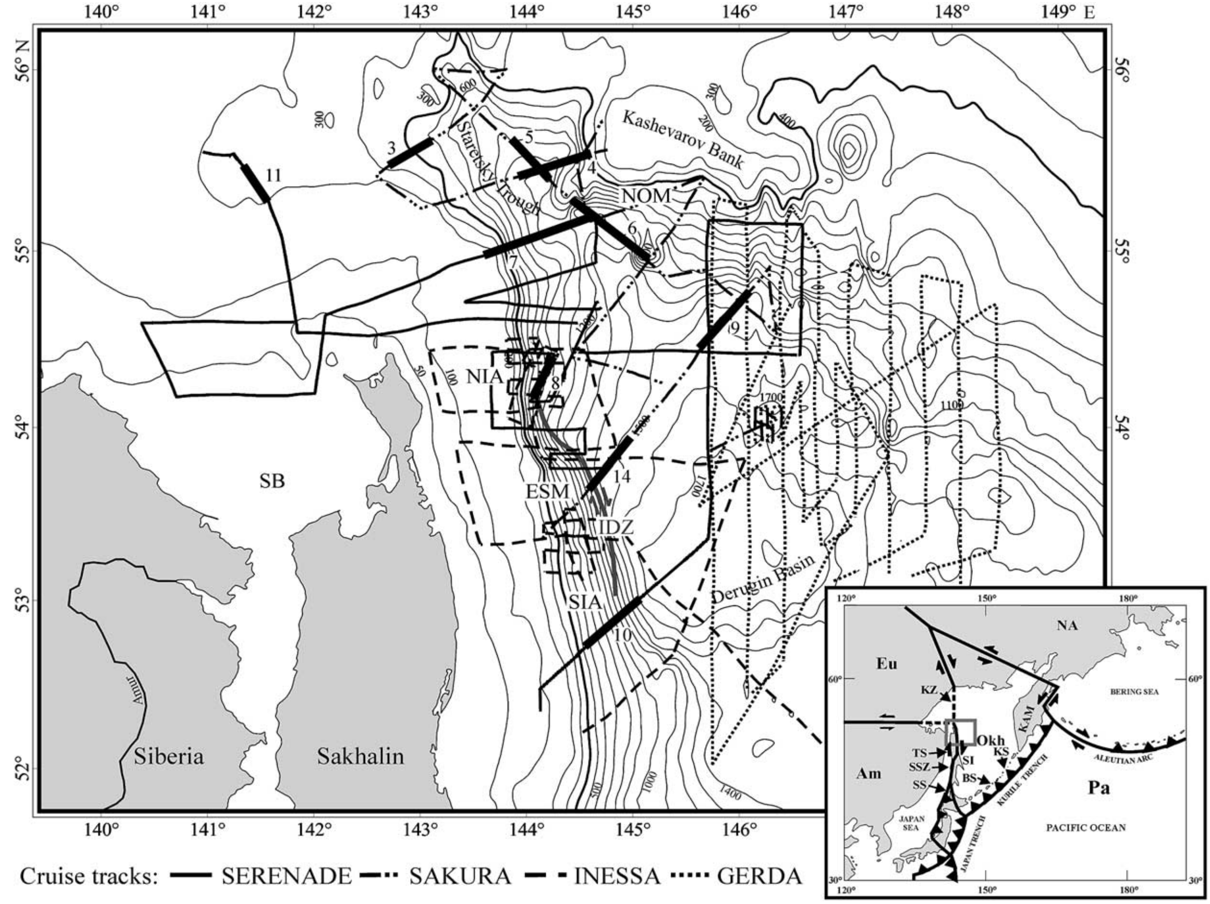

Fig. 1. Map of the northwestern Sea of Okhotsk study area showing the bathymetry, cruise tracks and location of profiles depicted in later figures (figure numbers are shown). The isobaths are drawn using data from NGDC (National Geophysical Data Center), GEBCO, ETOPO5 and our own cruises. Inset shows the location of the northwestern Sea of Okhotsk and the recent plate boundaries of the northwestern Pacific. The Okhotsk plate corresponds to the Sea of Okhotsk and parts of the adjacent land. Toothed lines mark subduction zones and lines with arrows strike-slip boundaries. BS = Bussol Strait, KS = Kruzenshterna Strait, SS = Soya Strait, TS = Tartar Strait, KAM = Kamchatka, SI = Sakhalin Island, IDZ = Inessa Deformation Zone, NOM = North Okhotsk margin, ESM = East Sakhalin margin, NIA = Northern Inessa Area, SIA = Southern Inessa Area, SB = Sakhalin Bay. Plates: Pa = Pacific, NA = North American, Eu = Eurasian, Am = Amur, Okh = Okhotsk. Shear zones: KZ = Kashevarov Zone, SSZ = Sakhalin Shear Zone.

Bank is generally flat, featureless, and less than 200 m in depth, leading to the suggestion that it originated by subaerial erosion (Gnibidenko and Khvedchuk, 1982). The Derugin Basin is outlined by the 1500 m isobath. It has a gentle but distinct bottom relief, which is largely a reflection of rotated block structures in the basement.

Although studies on the tectonics, paleoclimate, and stratigraphy of the sedimentary column have been carried out in the Sea of Okhotsk using seismic reflection profiling, and water and sediment sampling (e.g. Gnibidenko and Khvedchuk, 1982; Zhuravlev, 1984; Rodnikov et al., 1996; Worrall et al., 1996; Kononov et al., 1998), they are concentrated largely in the central and southern parts. The northwestern sector, especially the processes that controlled sedimentation there, are still little known. In this paper, we report on new data obtained under the German–Russian cooperative project KOMEX (*K*urile–*O*khotsk *M*arine *Ex*-

periment) and discuss their implications regarding sedimentation and its controlling factors in the northwestern Sea of Okhotsk (Fig. 1).

2. Oceanographic setting

The Sea of Okhotsk is a marginal sea enclosed on all sides by land or islands (Fig. 1). Water exchange with the Japan Sea occurs via the shallow Soya (40 m sill depth) and Tartar straits (10 m sill depth) (Favorite et al., 1976). Salt flux through these straits increases the density of the shelf waters in the Sea of Okhotsk (Talley, 1991). Exchange with the North Pacific takes place through the Bussol Strait (2300 m sill depth) and the Kruzenshterna Strait (1900 m) between the Kurile Islands (Fig. 1). The general surface circulation pattern in the Sea of Okhotsk is dominated by a basin-wide cyclonic gyre (Yang and Honjo, 1996; Shiga and Koizumi, 2000). North Pacific waters enter through the Kruzenshterna Strait, flow counterclockwise around the sea and exit through the Bussol Strait (Kitani, 1973; Favorite et al., 1976; Alfultis and Martin, 1987; Talley and Nagata, 1995).

Bottom currents in the northwestern Sea of Okhotsk are as yet not well-studied. They form largely by thermohaline convection that accompanies sea-ice formation in the winter, especially on the North Okhotsk shelf (Freeland et al., 1998). Ice formation and the subsequent brine release produce cold, dense, saline waters to form a basin-wide sub-zero dichothermal layer that extends between depths of 50 and 150 m (Kitani, 1973; Talley and Nagata, 1995; Yang and Honjo, 1996). These waters sink to a depth of about 600 m (in accordance with its density) as a gravity-driven slope current, and spread out laterally (Wong et al., 1998; Gladyshev et al., 2000). The dichothermal layer, however, is replenished during winter convection (Yang and Honjo, 1996). In this manner, the Sea of Okhotsk participates in the formation of oxygen-depleted North Pacific Intermediate Water (NPIW; Talley, 1991; Freeland et al., 1998). The oxygen-rich Sea of Okhotsk Intermediate Water (SOIW), found between depths of 200 and 1000 m (Wong et al., 1998), flows into the Pacific Ocean and ventilates the Pacific subpolar gyre (Talley, 1991; Freeland et al., 1998).

Vertical convection is enhanced by tides in the Sea of Okhotsk (Leonev, 1960; Kitani and Shimazaki, 1971; Kitani, 1973; Gladyshev, 1995). The tidal effect is significantly increased with sea-ice formation, when the wind-driven current regime is replaced by a tidally driven regime. Tidal currents cause vertical mixing, especially over bathymetric highs or flow constrictions such as on the North Okhotsk shelf or the Kashevarov Bank (Kowalik and Polyakov, 1998, 1999; Polyakov and Martin, 2000). In turn, vertical mixing transports heat to the sea surface, resulting in ice melting and polynya formation in the winter (Shevchenko and Putov, 1999; Polyakov and Martin, 2000). The accompanying decrease in surface salinity and increase in water column stability, however, is overwhelmed by the increase in surface density due to heat loss to the atmosphere (Polyakov and Martin, 2000). Thus, convection and a clockwise, density-driven, residual tidal current result. West winds over the North Okhotsk shelf keep the polynyas open. Over the Kashevarov Bank, tidally induced current velocities reach 264 cm/s at the surface, 177 cm/s at 80 m depth, and 164 cm/s at the bottom (Kowalik and Polyakov, 1999; Rogachev et al., 2000), and are high enough to cause erosion. Off the east coast of Sakhalin down to depths of about 900 m, southward-directed contour currents reach velocities of 30–35 cm/s in the winter (Mizuta et al., 2001).

3. Methods

The new data reported here consist of 8443 line-km of air gun seismic reflection profiles from four cruises: the GERDA cruise of 1996 (3020 line-km of single-channel analog data, cruise 16 of the R/V *Professor Gagarinsky*); the INESSA cruise of 1998 (1969 line-km of eight-channel digital data, cruise 22 of the R/V *Professor Gagarinsky*), the SAKURA cruise of 1999 (1356 line-km of eight-channel digital data, cruise 26 of the R/V *Professor Gagarinsky*) and the SERENADE cruise of 2001 (2098 line-km of eight-

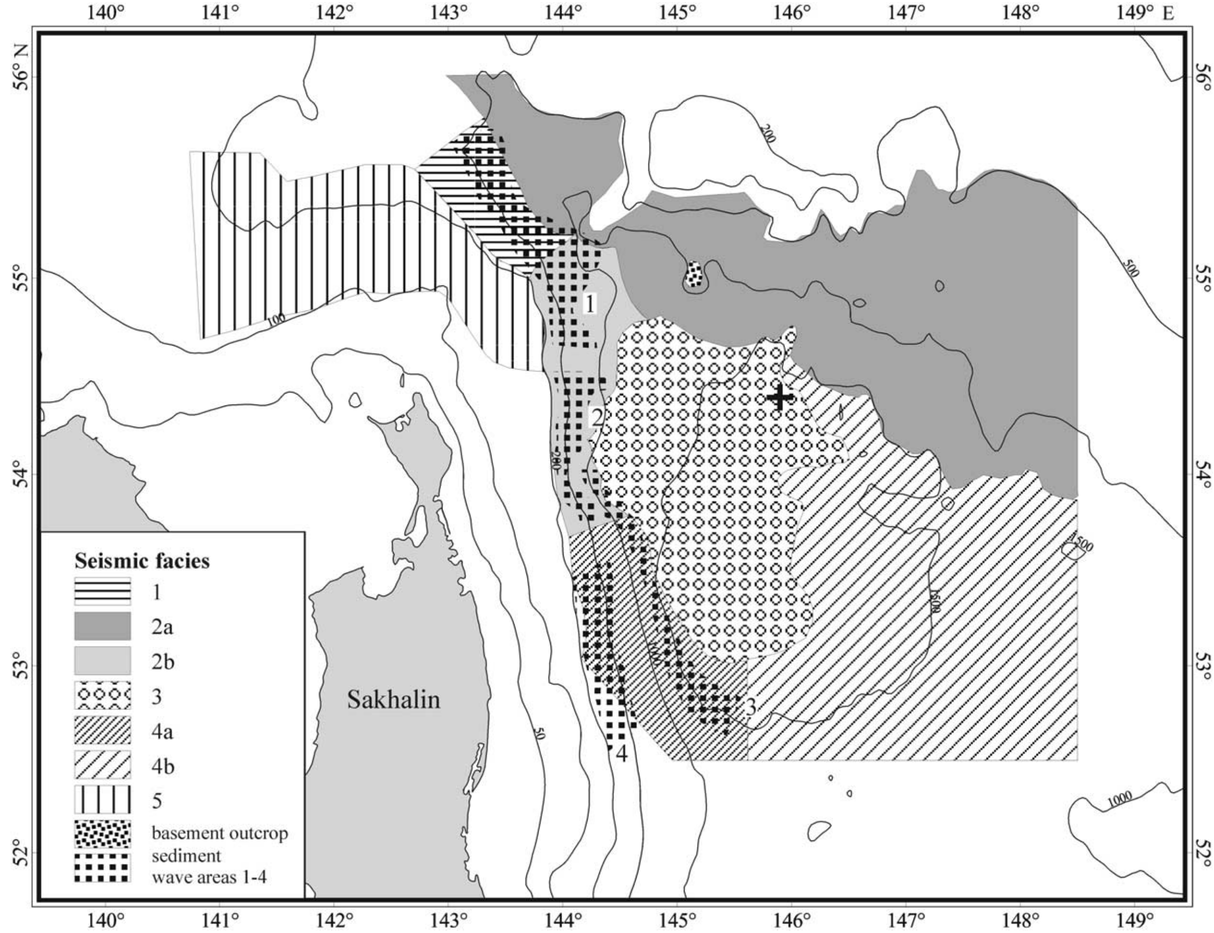

Fig. 2. Seismic facies distribution in the northwestern Sea of Okhotsk. The facies are: 1, chaotic; 2, well-stratified, wavy (2a, mound-like; 2b, lenticular); 3, massive, reflector-poor; 4, well-stratified, mostly even (4a, in the SIA; 4b, basinal subfacies); 5, prograding clinoform facies. The areas 1–4 with sediment waves are also shown. See text for discussion. Cross gives the position of core GE-99-31-3.

channel digital data, cruise 32 of the R/V *Professor Gagarinsky*). In addition, 1150 km of 3.5 kHz pinger profiles was acquired during the INESSA cruise and 1356 line-km of chirp profiles was obtained during the SAKURA cruise.

For the last three cruises, the seismic system used consisted of an air gun array and an eight-channel Geco-Prakla mini-streamer with a total active length of 100 m. In waters shallower than about 200 m, a mini-GI gun pressurized at 150 bar was triggered once every 25 m. In deeper waters, either a mini-GI gun (1.44 l) and a standard GI-gun (3.36 l), both configured in the harmonic mode, or a mini-GI gun in the harmonic mode combined with a standard GI-gun in the true GI mode were used. The seismic data were recorded digitally and later processed with a commercial software package.

Our sediment facies interpretations of the seismic facies types are based on KOMEX cores obtained and analyzed by colleagues from GEOMAR (Kiel), the Pacific Institute of Oceanology (Vladivostok), the P.P. Shirshov Institute of Oceanology (Moscow), and the Far East Geological Institute (Vladivostok) (Astakhov et al., 2000; Biebow and Hütten, 1999; Biebow et al., 2000; Gorbarenko et al., 2000; Kaiser et al., 2002; Leskov et al., 2000; Nürnberg et al., 1997, 2002a,b;

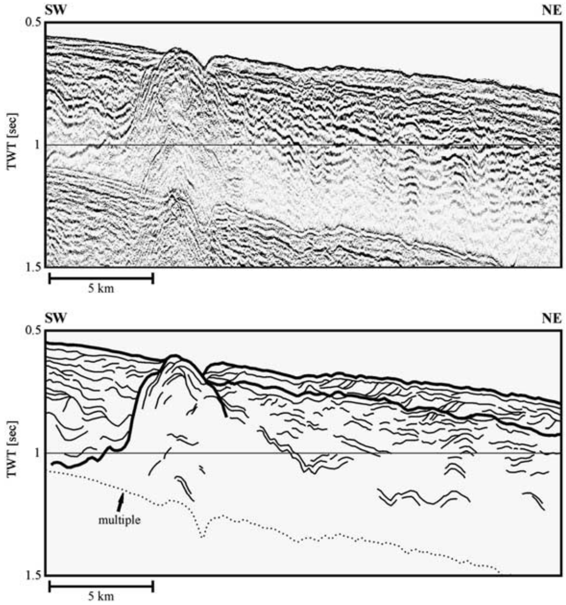

Fig. 3. Part of reflection seismic profile Sa9, SAKURA cruise, with interpreted section, showing the chaotic facies with chaotic to hyperbolic, occasionally wavy, subparallel reflections. See Fig. 1 for profile location.

Tiedemann et al., 2002). The core stations that lie within our study area are shown in the inset of Fig. 12.

4. Seismic facies of surficial and near-surficial sediments

Our seismic reflection data from the northwestern Sea of Okhotsk show a number of distinct surficial and near-surficial seismic facies, each of which is interpreted to result from a specific sedimentary environment (Fig. 2).

4.1. Chaotic facies (1)

The chaotic facies is found on the northernmost Sakhalin slope between 250 and 700 m water depth. It is characterized by chaotic to hyperbolic, occasionally wavy, subparallel reflections (Fig. 3). Large sediment waves, megaripples and giant foreset bedding are also common. This facies is interpreted to have formed under the influence of intense bottom currents, and is represented by coarse, reworked sediments. It may also represent reworking by strong bottom currents of mass wasting deposits (facies 5, see later) destabilized by motions associated with the nearby Kashevarov Zone (Fig. 1).

4.2. Well-stratified and wavy facies (2)

4.2.1. Subfacies 2a – mound-like

The well-stratified mound-like subfacies 2a is found on the northeastern flank of the Staretsky Trough and the slope of the North Okhotsk margin within a water depth of 400–1500 m (Fig. 2).

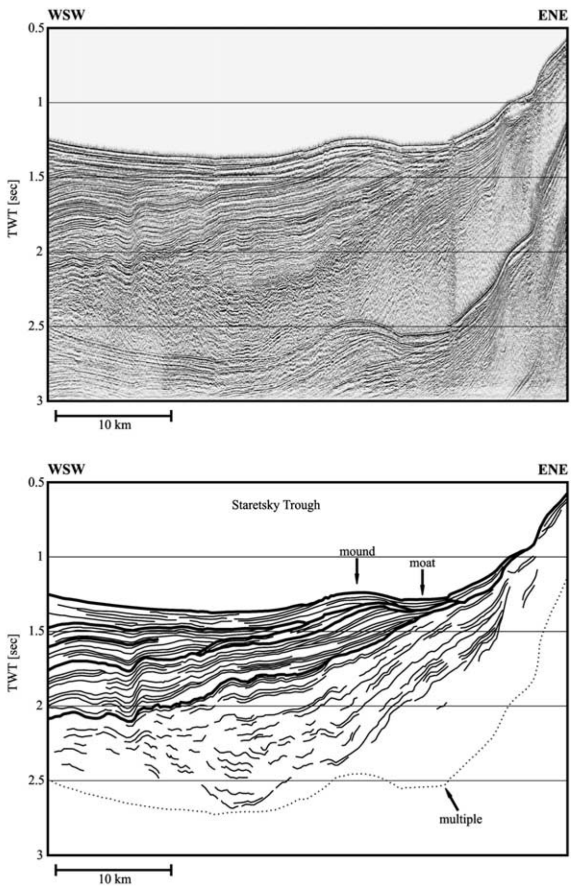

Fig. 4. Part of reflection seismic profile Sa11, SAKURA cruise, with interpreted section. Note the several generations of well-stratified, slope-plastered sheeted drifts that occur in the Staretsky Trough (seismic facies 2a), and the transition to mounded drifts accompanied by moats as the trough margin is reached. See Fig. 1 for profile location.

It consists of parallel to subparallel, well-stratified reflections with medium-to-high amplitudes (Figs. 4–6). The external geometry varies from sheet-like near the trough axis to mounded on the southern slope of the Kashevarov Bank (Fig. 4). The seismic facies characteristics of subfacies 2a and the widespread occurrence of internal erosional unconformities and moats suggest that this subfacies comprises drift sediments laid down between uplifted and tilted basement blocks under the control of bottom currents, with periods of erosion and non-deposition in between.

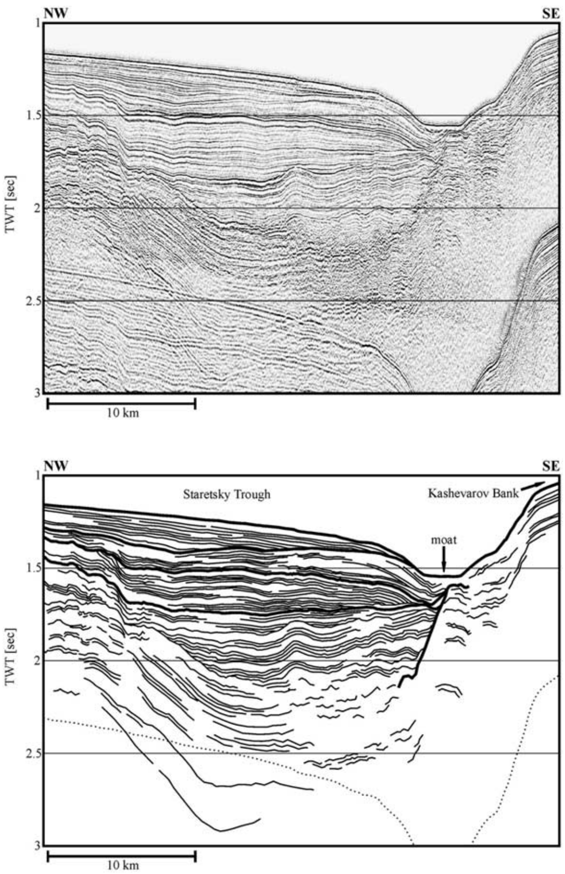

Fig. 5. Part of reflection seismic profile Sa7, SAKURA cruise, with interpreted section, showing three vertically stacked, separated elongate drifts oriented subparallel to the continental margin (seismic facies 2a). Note the moats at the base of the Kashevarov Bank and fault structures at the NW part of the section. See Fig. 1 for profile location.

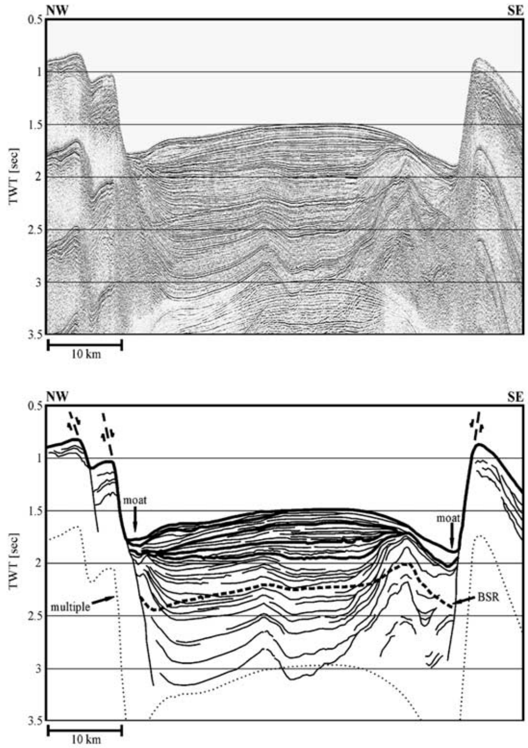

Fig. 6. Part of profile Sa7, SAKURA cruise, with interpreted section, showing confined drifts between exposed rotated basement blocks at a water depth of about 1100 m (seismic facies 2a). Confinement strengthens the current flow. Boundary moats form at the blocks while a large mounded drift develops between the blocks. The BSR is dashed. See Fig. 1 for profile location.

4.2.2. Subfacies 2b – lenticular

Subfacies 2b is confined to the northernmost upper slope of the Sakhalin margin within the depth range of 200–1000 m (Fig. 2). It is characterized by continuous, low-to-medium amplitude, well-stratified, wavy reflections and a lenticular external shape (Figs. 7 and 8). Here, in contrast to subfacies 2a, sediment waves occur either at the seafloor or are occasionally buried under well-stratified sediments. We interpret this seismic facies to represent a separated elongate drift laid down under alongslope bottom currents (Fig. 7). In the south, it directly overlies a small slope fan with a channel-levee system (Fig. 8), pointing to the close interplay between downslope and alongslope processes.

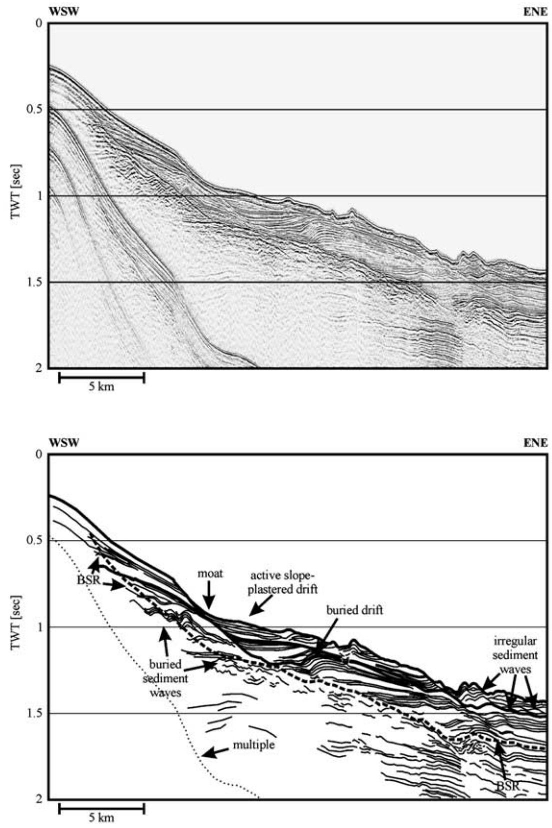

Fig. 7. Part of reflection seismic profile Se17, SERENADE cruise, with interpreted section, showing a plastered drift body of seismic facies 2b and sediment waves of area 1. See Fig. 1 for profile location.

4.3. Massive, reflector-poor facies (3)

This facies occurs in the western Derugin Basin and on its northwestern margin (Fig. 2). Its transition to subfacies 2b to the northwest is gradual, but is abrupt to the well-stratified sediments to the southwest (Fig. 2). To the east and the northeast, this facies pinches out in the form of tongue-like structures, resulting in facies interfingering (Fig. 9).

The massive, reflector-poor facies is characterized by incoherent discontinuous reflections and hence a lack of internal structure. In places, medium-to-high amplitude subparallel reflections occur. The spatial distribution and seismic characteristics of this facies suggest that it may represent mass wasting deposits, namely debris flows and slumps, giving way to turbidites in the extreme distal zone (Haq, 1998; van Weering et al., 1998). The turbiditic character is documented in core GE 99-31-3 (location in Fig. 2), in which turbidites were recovered at core depths >5.6 m (age >130 kyr) (Astakhov et al., 2000).

4.4. Well-stratified, even facies (4)

4.4.1. Subfacies 4a – Southern Inessa Area (SIA)

The well-stratified, largely even subfacies 4a consists of regular, parallel, high-amplitude reflections and is found on the SIA of the Sakhalin margin (Figs. 2 and 10). Its slightly downslope-divergent internal reflection pattern suggests a differential subsidence that increases basinward, but the ramp margin without a distinct shelf break indicates that sedimentation has kept pace with this subsidence. On the upper slope this subfacies is represented by sediment waves at the seafloor. Its transition to the massive, reflector-poor facies is sharp and might be marked by the Inessa Deformation Zone (IDZ; Fig. 1).

4.4.2. Subfacies 4b – basinal setting

Subfacies 4b (not illustrated) is found in the eastern Derugin Basin (Fig. 2). It comprises con-

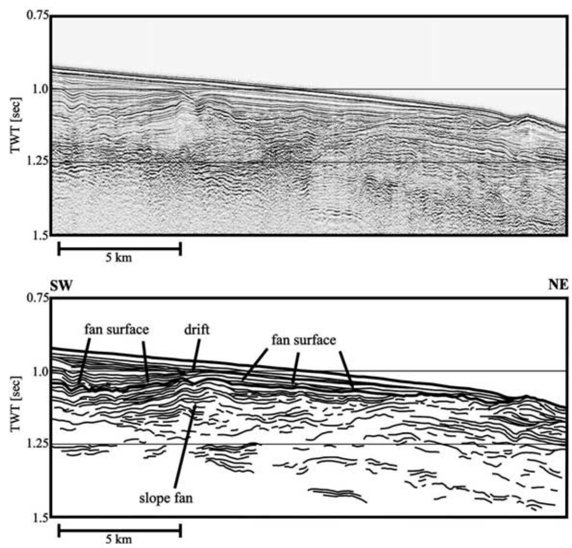

Fig. 8. Part of reflection seismic profile Se23, SERENADE cruise, with interpreted section, showing a slope fan covered by recent drift sediments. See Fig. 1 for profile location.

tinuous, parallel-to-subparallel reflections with high-to-medium amplitudes. Because of large distances to the depocenters at the continental margin, this seismic subfacies probably consists mainly of hemipelagic deposits with ice-rafted detritus (IRD) (Biebow et al., 2000; Gorbarenko et al., 2000). A prominent bottom simulating reflector generally accompanies this facies type.

4.5. *Prograding clinoform facies (5)*

This facies, sometimes overlain by migrating sediment waves, is represented by medium-amplitude, oblique-tangential (up to 10°), northward-prograding clinoforms that terminate upslope with toplap and basinward with downlap (Fig. 11). It occurs at about 220 m water depth on the North Sakhalin margin (Fig. 2). We interpret this facies to represent a high-energy depositional environment characterized by high sediment supply, little or no basin subsidence and a sea-level stillstand. Basinward progradation of the offlap break suggests a regression of the shoreline. This, together with sediment bypassing of the shelf and the clinoform architecture of the reflectors, indicate that this facies marks perched, prograding shelf edge lowstand wedges of the River Amur. Vertical stacking of several generations of

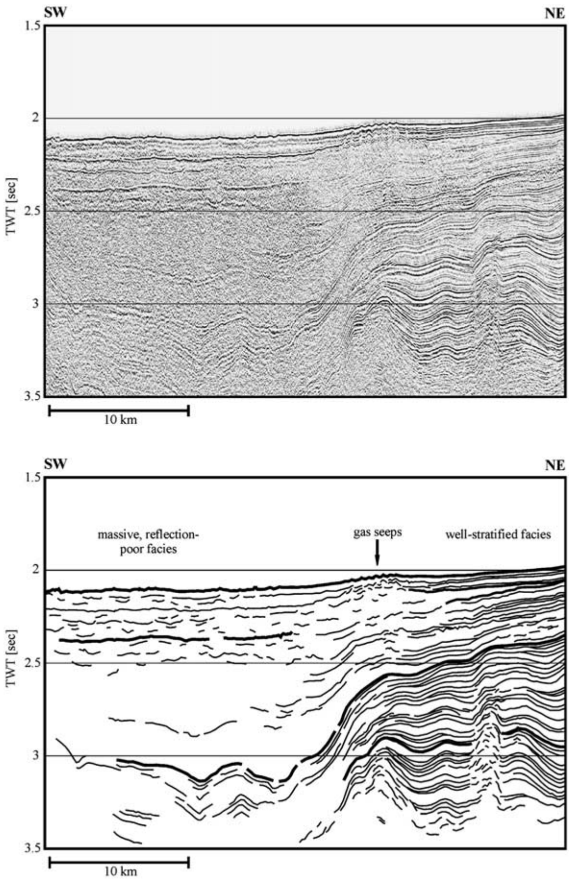

Fig. 9. Part of reflection seismic profile Sa3, SAKURA cruise, with interpreted section. Note the almost structureless, massive, reflector-poor facies 3, the well-stratified facies 2a, and pinch-out of the former within the latter. See Fig. 1 for profile location.

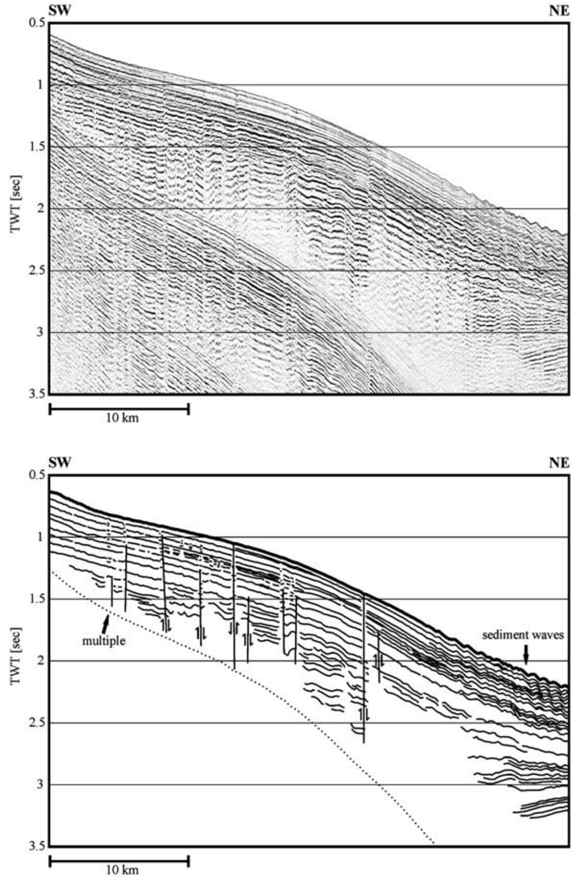

Fig. 10. Part of reflection seismic profile Se5, SERENADE cruise, with interpreted section, showing the well-stratified, largely even subfacies 4a with regular, parallel, high-amplitude reflections. Vertical lines mark interpreted faults. See Fig. 1 for profile location.

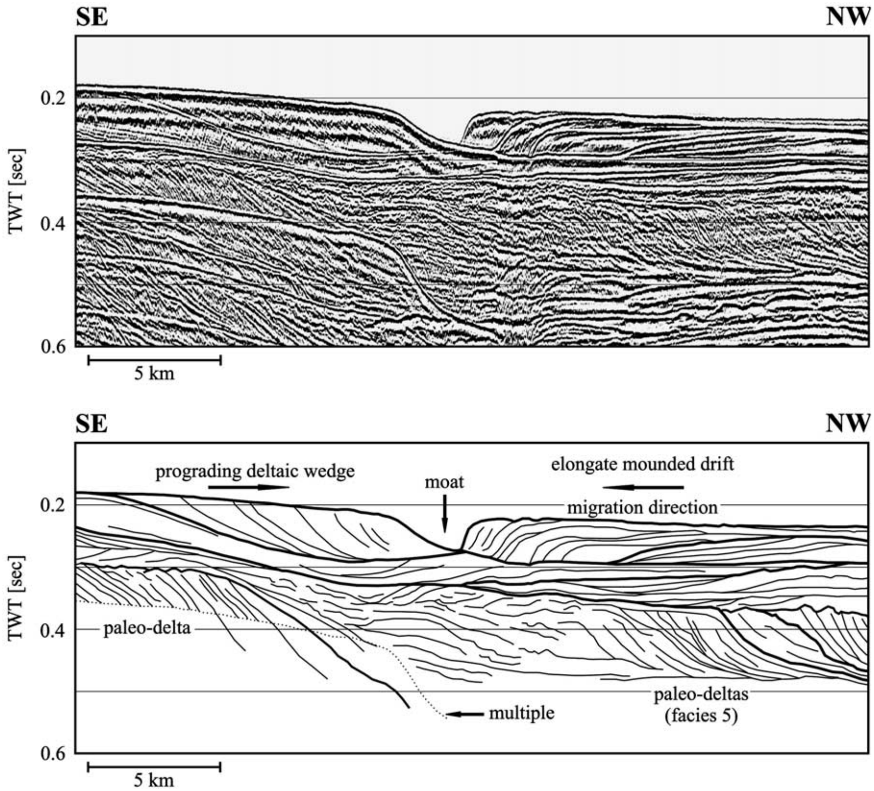

Fig. 11. Part of profile Se11, SERENADE cruise, with interpreted section, showing an elongate mounded drift on the slope north of Sahkalin Island. It progrades upslope, the direction in which the dip of the internal reflectors at its frontal zone gradually increases. The drift body is underlain by downslope-prograding lowstand deltaic wedges (seismic facies 5). See Fig. 1 for profile location.

delta wedges implies repeated deposition over several sea-level cycles (Fig. 11).

5. Discussion

5.1. Bottom current-controlled sedimentation

5.1.1. General

Sedimentation at continental margins is often influenced by the complex interaction between gravitational downslope and current-controlled alongslope transport mechanisms. Such interactions have been described on passive continental margins such as those in the Atlantic (Hollister and Heezen, 1972), the Indian Ocean and around the Antarctic (Harris et al., 2001), as well as on active margins such as in the Sumba Basin and near New Zealand (Reed et al., 1987; Fulthorpe and Carter, 1991; Carter and McCave, 1994). The influence of bottom currents on sediment accumulation and erosion at the seafloor is particularly strong in areas where a highly complex bottom morphology leads to a deflection or focusing of these currents and with it an intensification of the flow (Stoker, 1998).

In general, contourite drifts are lenticular with an upper boundary that is convex upward, and a lower boundary that can represent basin-wide erosive unconformities (Faugères et al., 1999). Based on morphostructure and the hydrodynamic regime at the time of sedimentation, four different types of contourite drifts have been recognized. These are: contourite-sheeted drifts, elongate-mounded drifts, channel-related drifts, and confined drifts (Faugères et al., 1993a,b, 1999). Sediment waves, sometimes grouped into wave fields, can also result from bottom current activity (Faugères et al., 1999).

5.1.2. Drift sediments

Well-stratified, predominantly silty sediment bodies (Astakhov et al., 2000) interpreted as slope-plastered sheeted drifts occur in the Staretsky Trough (subfacies 2a; Figs. 4–6). They formed under the influence of tidally induced, descending and outwardly spreading bottom currents with moderate intensities. Their thickness is uniform and their internal reflections typically have medium continuity and medium amplitude. They are in places semi-transparent, and are occasionally superposed by fields of complex sediment waves as in the Atlantic (Faugères et al., 1993a,b, 1999).

Near the Kashevarov Bank, the sheeted drifts give way to separated elongate drifts that are oriented subparallel to the continental margin. Profile Sa7 (Fig. 5) shows a drift complex consisting of three stacked lenticular drift bodies, each marked by a moat at the base of the Kashevarov Bank. These bodies are separated by major erosional unconformities (see Fig. 12) that characterize the transitions (from erosion/non-deposition to deposition) that result from episodic changes in the bottom current regime, with the base of each drift body marking the onset of significant bottom currents. The upward and oblique stacking of the drift units suggests differences in the bottom current regimes at different times. The elongated form becomes more prominent as the bottom currents are more focused where the trough cross-section decreases or where tilted basement blocks deflect the water flow.

Fig. 11 shows a particularly interesting example of an elongate mounded drift on the slope north of Sahkalin Bay at water depths between 200 and 340 m. It is developed on a major unconformity and progrades southward upslope (opposite to the direction of lowstand deltaic propagation, see facies 5). The dip of the internal reflectors at its frontal zone increases gradually upslope in a manner analogous to the Feni drift on the northeastern margin of Rockhall Trough (Stoker, 1998; Faugères et al., 1999). It is deposited under a strong alongslope bottom current regime in which erosion and sediment reworking dominate.

Mounded confined drifts accompanied by moats occur between exposed rotated basement blocks at water depths generally less than 1000 m (Fig. 6). At these locations, because the current flow is strengthened and confined to the area between the blocks, boundary channels (moats) are formed at the blocks while large mounded drifts are deposited between the blocks (moat locations generally coincide with the location of the schematic thermohaline bottom current west and south of Kashevarov Bank in Fig. 12). At water depths >1000 m, drift sedimentation decreases and mass wasting or hemipelagic sedimentation sets in. However, buried paleo-drifts can be found up to a present-day water depth of about 1500 m. Generally, there is a landward displacement of these drift bodies (and hence of their basal regional unconformities) over the time period covered by our seismic profiles.

Farther south in the SIA, drift sedimentation is no longer dominant, probably because of reduced flow as a result of a substantial decrease in the slope gradient, general widening of the seabed (see the 1300 m isobaths on either side of Derugin Basin), and a possible eastward deflection of bottom currents by the basin flanks at 1500–1700 m depths just south of the SIA (Fig. 1).

5.1.3. Sediment waves

A prominent feature on the northern Sakhalin margin is sediment waves. These waves are formed under bottom current or tectonic control (Fig. 2; Faugères et al., 1999; Masson et al., 2002), and are found in four areas on the continental slope.

The sediment waves in area 1 are interpreted as contourite waves (Fig. 2). They are found within water depths of 300–1100 m, and have wavelengths of 380–800 m and amplitudes of 10–35 m (Fig. 2). Their migration varies from slightly upstream to slightly downstream; standing waves also occur. While they do not show any regular downstream changes in dimension and depositional geometry, distinct irregular geometry variations within the stratigraphic column are common. Some of these sediment waves are surficial and possibly active, others are buried under sediments (Fig. 7).

Area 2 is characterized by sediment waves with wavelengths of 400 to > 800 m and amplitudes of 10–20 m (Fig. 2). They are confined to water depths of 300–1100 m. Both their wavelengths and amplitudes increase upslope in the direction of wave migration. Generally, these sediment waves are buried, indicating that they are no longer active. They are probably formed by slope-parallel currents. However, a tectonic origin associated with recent activity of the IDZ (Fig. 1) cannot be ruled out in view of mass wasting in the NIA (see Section 5.2). They may have formed during an early event and are now being buried in a period of reduced mass wasting.

Typical for area 3 on the Sakhalin continental rise between depths of 900 and 1600 m are more-or-less slope-parallel, upslope-migrating sediment waves of 400–1200 m wavelength and 15–20 m amplitude with sinuous or curvilinear crests (Fig. 2). Their amplitudes and wavelengths decrease with decreasing slope gradient. We suggest that they are either slope sediment ridges associated with compressional movements along the IDZ of the southwestern Derugin Basin, or they represent translational slides which appear in profile as upslope-migrating waves (e.g. Barnes and Lewis, 1991).

Sediment waves of area 4 are surficial and quasi-symmetric, with wavelengths of about 500 m and amplitudes of around 15 m (Fig. 2). They strike parallel to the continental slope, are confined to a depth range of 200–700 m, and have a sinuous geometry. The lack of a distinct migration trend suggests that they probably originated from the action of contour currents rather than turbidity currents.

5.2. The depositional regime during drift sedimentation

Sedimentation in the northwestern Sea of Okhotsk during drift formation is controlled largely by fluvial input of the Amur River and by bottom currents. Both of these factors are a function of the ice cover. During interglacials such as today, in the winter 75% of the Sea of Okhotsk, including its entire northwestern sector, is covered by sea ice averaging 1 m in thickness. In the summer, the sea is ice-free. During glacial winters, the Sea of Okhotsk was completely covered by ice; during the glacial summers, the sea-ice boundary retreated probably to about 54°N (Kaiser et al., 2002; Nürnberg et al., 2002a). Glaciers were restricted to the higher mountains (Hopkins, 1972; Frenzel et al., 1992) because the climate of Siberia was too dry to support the development of a large ice cap (Morley et al., 1991). This is corroborated by the lack of $\delta^{18}O$ anomalies in cores that would indicate meltwater input during deglaciation (Gorbarenko et al., 1990; Gorbarenko, 1991). Also, microfossil data are consistent with a model of glacial winter ice cover and incomplete summer mixing (Sancetta, 1983). We presume that in our study area, a perennial ice cover persisted during glacial periods (Leskov et al., 2000), with the exception of polynyas and possibly the southern Derugin Basin. This would imply that surface circulation was significantly reduced while loss in bottom circulation may be partly compensated by an enhanced generation of SOIW and of bottom water through under-ice cooling (in a way similar to that occurring under ice shelves in the Weddell and Ross seas of Antarctica).

The abundance of the planktonic radiolarian *Cycladophora davisiana* in the southern Sea of Okhotsk during the last glacial maximum (LGM) is, in contrast to the open ocean, lower than their Holocene values (Morley et al., 1991). This is interpreted to imply higher surface salinities (drier climate) and lower sea-surface temperatures (SSTs) during the LGM, and with it an increase in vertical convection during glacial times. $\delta^{13}C$ values measured on epibenthic foraminifers increased during the LGM. This suggests better ventilation of the water masses and/or enhanced formation of SOIW (Keigwin, 1998), again implying an enhanced vertical convection.

During the interglacials, starting with snowmelt and in sea ice-free conditions, the Amur River transports suspended load as over- or interflows into Sakhalin Bay (Fig. 12). Here, mixing with seawater causes the water mass to sink and the fluvial sediment particles are eventually drawn

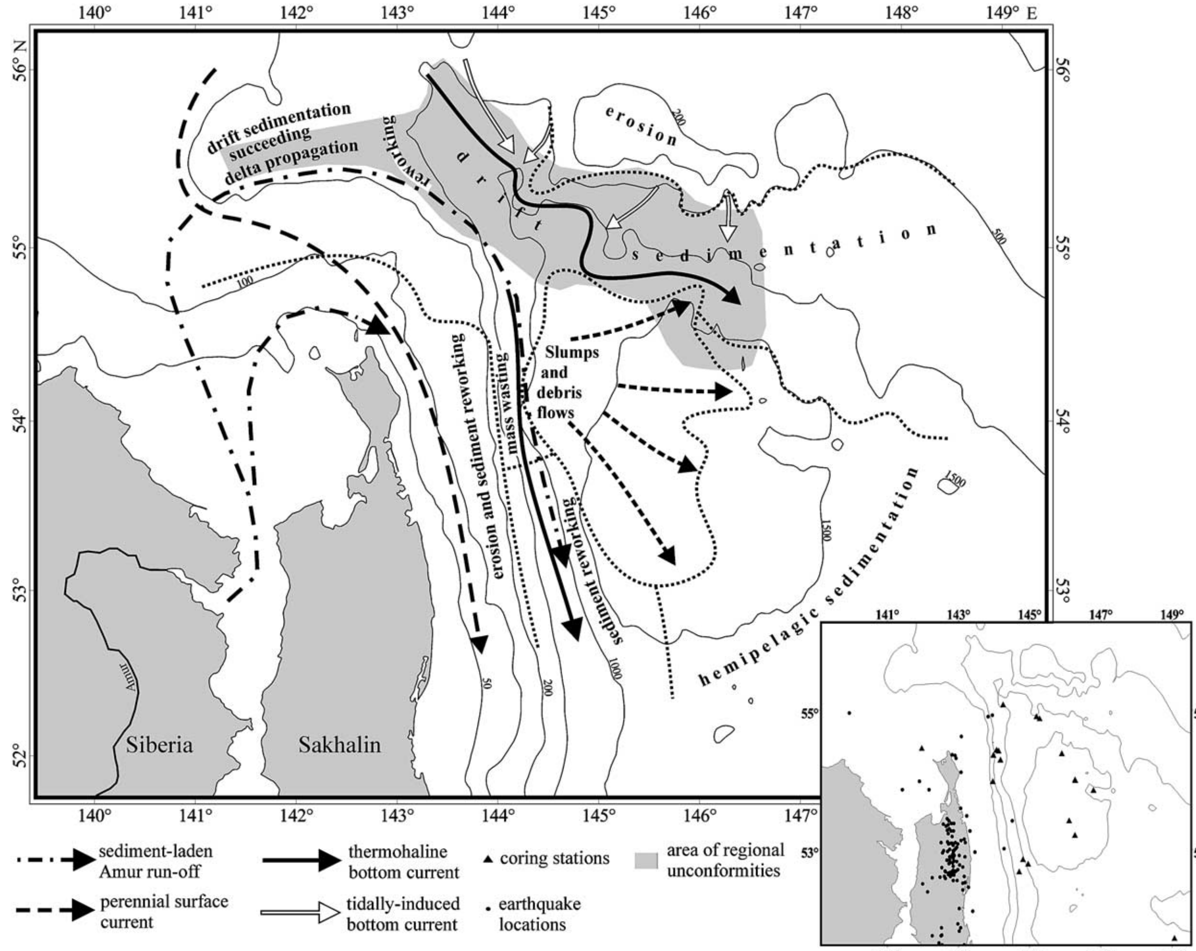

Fig. 12. Schematic map of the dominant Plio–Quaternary sedimentation processes in the northwestern Sea of Okhotsk. The schematic bottom currents reconstructed from the drift deposits and from areas of erosion and sediment reworking are also shown. Their origin is presumably thermohaline as well as tidally induced. The schematic sediment-laden Amur runoff during times without an ice cover and the year-round, cyclonal isobath-parallel surface currents are also shown. The extent of the basal regional unconformity marking the onset of drift sedimentation is shown in gray. Although the drift bodies and with them their (younger) lower unconformities migrate with time, this migration is not very large and therefore, for the sake of clarity, the distributions of the younger unconformities are not plotted. See text for further details. Inset: dots, earthquake epicenters for the period 1970–2002 from the U.S. Geological Survey (http://neic.usgs.gov/neis/epic/epic.html); triangles, core stations of the KOMEX project.

into the southward-directed near-bottom currents. They are transported together with detritus from the Siberian shelf into the Staretsky Trough, where the currents are deflected by the Coriolis force up the southwestern flank of the trough (Fig. 12). This leads to upslope erosion, downslope drift sedimentation, and up- and alongslope migration of the drift sediments. Our seismic profiles show that moats developed along the axis of Staretsky Trough and on the continental slope of the North Sakhalin margin (Fig. 12). These moats widen and flatten to the southeast and are found at a water depth of about 200 m at the western entrance of the trough to around 700 m on the northwestern slope of the Derugin Basin. They may represent residual space left between the landward-prograding offshelf sediment drift and the adjacent shelf foreslope (Fulthorpe and Carter, 1991). The bottom currents are directed oblique to the isobaths as a result of sinking of the cold dense water mass formed by brine release during the winter. The fine fraction of the fluvial sediments, however, is presumably deposited as a fan on the southern Sakhalin margin outside our study area.

During glacial periods, freshwater and sediment discharge of the Amur River is significantly reduced because the climate was much drier over most of East Asia (Morley et al., 1991; Tiedemann et al., 2002). The occurrence of polynyas along the coast of Siberia as well as over the Kashevarov Bank results in the formation of cold, dense, saline water masses which flow downslope as gravity-driven currents. The fluvial sediments are laid down partly as lowstand deltaic wedges north of Sakhalin Bay (Fig. 2, facies 5), and partly as giant confined drift bodies (Fig. 2, facies 2a) by thermohaline and tidally induced downslope transport (Fig. 12). As these downslope currents reach the floor of the Staretsky Trough, they flow down-trough until their density approximately equals that of the surrounding waters, when mixing and dispersion take over. On the northern Sakhalin margin, these currents might have generated the sediment wave fields in area 1 by eroding the floor of the trough axis and depositing the reworked sediments to the right of their flow direction (Fig. 2). There is, in addition, an important southward longshore drift as attested to by barrier–lagoon complexes along the coast and sediment waves on the shelf (Fig. 12).

Faugères et al. (1993a), Nelson et al. (1993) and Faugères et al. (1999) suggested that drift sediments commonly form: (1) during high or falling sea level, when turbidite sedimentation is low and therefore unable to mask the effects of bottom currents, or (2) during times of moderate bottom current intensity regardless of sea level. Specifically, they noted that there is no direct link between sea-level change and drift deposition at the glacial–interglacial time scale, contrary to the models of Haq (1991), Vail et al. (1991), and Posamentier et al. (1988). Rather, they suggest that the onset of contourite drift sedimentation is triggered by global oceanic events accompanied by increased bottom current activity and with it a large-scale surface of erosion or non-deposition in the drift system. Regional erosional unconformities underlie the stacked mounded contourite drift bodies in our study area (Fig. 12). After the cessation of major bottom circulation and contourite accumulation, hemipelagic and/or turbiditic sedimentation takes over. The oceanic events may be climatically controlled (changes in the extent of polar ice caps and sea ice) or tectonically controlled (opening and closing of sills and gateways).

An example of a global hydrological event is the inception of Quaternary glaciation. In the northern Pacific, it is accompanied by abrupt changes in $\delta^{18}O$ and a sudden onset of IRD deposition interpreted to be the result of an increase in the vigor of deep-sea circulation and an intensification in mixing of the water masses at 2.5 Ma (Rea and Schrader, 1985; Rea et al., 1993). Maslin et al. (1996) reported a dramatic increase in IRD coeval with a drastic drop in SST at ODP site 882 about 180 km east of Kamchatka at 2.75 Ma. They concluded that this marks an intensificaton of northern hemisphere glaciation that was accompanied by changes in deep-ocean circulation. Kwiek and Ravelo (1999) concluded from benthic foraminiferal stable isotope data that thermohaline overturning was more rapid, and formation of warmer, saltier intermediate water was more enhanced in the northern Pacific during the warm period of the early Pliocene (2.7 Ma). Since the northwestern Sea of Okhotsk plays an important role in the formation of intermediate and deep waters in the North Pacific, similar hydrographic changes must also have occurred there. Thus, it may be assumed that the onset of drift sedimentation in the northwestern Sea of Okhotsk was at about 2.7 Ma. Because the base of the paleo-drift deposits observed lies commonly 300–600 m below the seafloor, the average computed sedimentation rate for the past 2.7 Myr would be 11–22 cm/kyr. This rate is compatible with rates measured directly from cores for the past 350 kyr, which are 50–140 cm/kyr on the Sakhalin slope and 2–5 cm/kyr in the central Sea of Okhotsk during the Holocene, and 25–50% lower during glacial times (Gorbarenko et al., 1990; Biebow et al., 2000; Nürnberg et al., 2002b; Tiedemann et al., 2002). Also, because the younger regional unconformities have not been drilled or cored, their ages and the cause of the strong bottom flows responsible for them remain unknown.

5.3. Sediment mass wasting

Mass wasting due to slope instability has been widely reported in the literature (e.g. Rothwell et al., 1998; Vogt et al., 1999; Kuipers et al., 2000; Laberg et al., 2002). For example, Bugge et al. (1987) and Evans et al. (1996) reported six large-scale sediment slide events in the Storegga Slide region west of Norway. Analogously, Rothwell et al. (1998) demonstrated that catastrophic submarine slope failures resulted in the deposition of megaturbidites during the late Pleistocene in the western Mediterranean. Possible triggering mechanisms suggested for these events include: (1) rapid sedimentation, which leads to slope over-steepening and pore water over-pressuring, (2) gas release from gas hydrates caused by a reduction of the confining pressure as a result of lowered sea level, and (3) earthquakes (Bugge et al., 1987; Kayen and Lee, 1993; Rothwell et al., 1998; Mienert and Posewang, 1999).

The massive, reflector-poor facies observed in the western Derugin Basin is characterized by a number of internally homogeneous, vertically stacked units, each typically a few tens of meters in thickness. These units are separated from one another by one or more continuous reflectors of intermediate amplitude (Fig. 9). They have the geometry of an onlapping fill or occasionally a basin floor fan (with downlap terminations both up- and downslope). We interpret these units to represent individual debris flows or slump events, and the reflectors between them IRD-bearing, hemipelagic sediments deposited between such events (Biebow et al., 2000).

We speculate that the mass wasting deposits (massive, reflector-poor facies) are derived from the upper slope of the northern East Sakhalin margin, possibly from the NIA. The slope cross-section here has a pronounced concave form, the average gradient being 2.5° (Fig. 13a). The transition to the shelf is marked by a distinct shelf break at about 200 m water depth. In contrast, the ramp margin to the south (the SIA) is characterized by a convex cross-section with an average gradient of only 1.5°, and the lack of a recognizable shelf break (Fig. 13a). From the shelf edge to a depth of about 1100 m on the lower slope, the slope cross-sections of the NIA and SIA differ by a more-or-less constant amount (shaded in gray in Fig. 13a). Assuming that the original margin morphologies were similar, repeated sediment slumping and debris flow must have occurred in the NIA to produce this cross-sectional difference. Large sediment packets must have been torn from the slope and deposited in the Derugin Basin. Assuming that a 70 km longitudinal section of the continental slope is involved

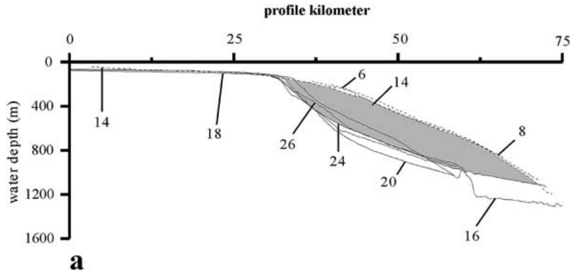

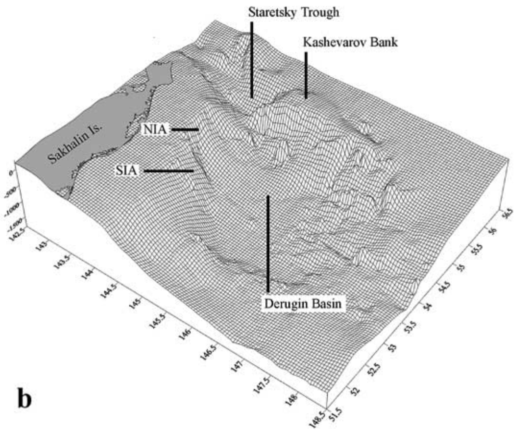

Fig. 13. (a) Comparison between present-day stacked bathymetric profiles from the NIA (profiles 18, 26, 24 and 20 from N to S, INESSA cruise; see Fig. 1 for locations) and the SIA (profiles 6, 14 and 8), showing that the slope cross-sections from the shelf edge to a depth of about 1100 m differ by a more-or-less constant amount (gray). (b) Block diagram of the northwestern Sea of Okhotsk showing the contrast in bottom relief between NIA and SIA.

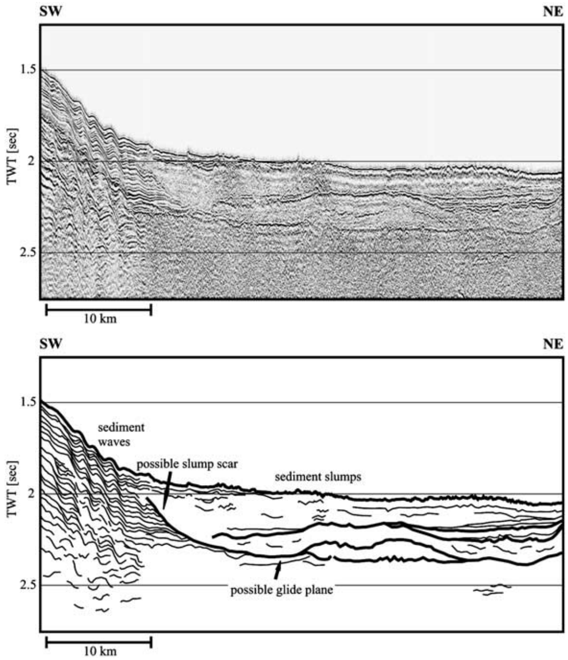

Fig. 14. Part of reflection seismic profile Sa3, SAKURA cruise, with interpreted section. A possible slump scar and glide plane, as well as two sediment slumps are marked. See Fig. 1 for profile location.

in the last mass wasting events (Fig. 2), the volume of sediment lost would be about 660 km^3 (Fig. 12b; Elverhøi et al., 1997). We note that paleo-slump or slide scars (in the form of steep scarps that terminate normal stratifications) and glide planes are uncommon on our profiles (e.g. Fig. 14). However, this may be due to the fact that the number of profiles which reach onto the shelf is limited and that there is a scarcity of side-scan data.

In the northwestern Sea of Okhotsk, modern shallow seismicity is concentrated along the Sakhalin Shear Zone (Chapman and Solomon, 1976; Savostin et al., 1983; Seno and Sakurai, 1996). For the period 1970–2002, earthquakes, though infrequent, occurred in both the NIA and the SIA (Fig. 12, inset). However, they are very shallow (1–3 km) in the former area, and are considerably deeper (19–33 km) in the latter. This implies that earthquake-triggered slope instabilities are more likely in the NIA, consistent with our speculation that the NIA is the source area for the mass wasting deposits. We note that the age of the mass wasting events is presumably pre-Uppermost Pleistocene for two reasons. Firstly, the slumps and debris flows do not extend to the seafloor in our seismic profiles. Secondly, the isotopic and stratigraphic records of all cores obtained from the Sea of Okhotsk within the framework of the KOMEX project going back to about 350 ka are correlatable (e.g. Astakhov et al., 2000). We assume that the pre-Uppermost Pleistocene seismicity pattern is similar to that of the present.

Another possible triggering mechanism for mass wasting is gas release from gas hydrates during sea-level lowstands. Widespread gas hydrate occurrence in our study area is suggested by the existence of an ubiquitous BSR in our seismic profiles (Lüdmann and Wong, 2003). As sea level falls at the onset of a glacial period, the hydrostatic pressure at the BSR depth drops. Gas hydrates already formed at or near the BSR would become destabilized since the changed P–T conditions now lie outside the gas hydrate stability zone. The resulting gas release would decrease the shear strength of the sediments, eventually leading to slope instabilities, especially where the BSR outcrops at the seafloor. This triggering mechanism, however, does not explain why mass wasting is presumably centered around the NIA and not around the SIA, although a sea-level fall would affect both areas equally. We note in addition that triggering by over-steepening and/or pore-water over-pressuring due to rapid sedimentation and perhaps shallow gas occurrences in the IDZ cannot be ruled out.

6. Conclusions

Our seismic reflection data show that during the Quaternary, alongslope sedimentation processes controlled by strong bottom currents are prevalent in the northwestern Sea of Okhotsk. They give rise to contourite drifts and sediment waves represented by the seismic facies 1, 2a, 2b and 4a (Fig. 2). Their distribution in the northwestern Sea of Okhotsk is confined to the Staretsky Trough as well as the continental slopes south of the Kashevarov Bank and east of Sakhalin Island. These bottom currents are controlled by the oceanographic regime in the Sea of Okhotsk, which is probably closely linked to intermediate- and deep-water circulation patterns in the northern Pacific. The bottom currents are largely thermohaline in origin, but can also be induced by tides, especially on shelves and on the Kashevarov Bank. Drift deposits form within the depth range of 350–1000 m. Paleo-drifts, however, are found down to a present-day depth of 1500 m. The contourite drifts include slope-plastered sheeted drifts in the Staretsky Trough and on the northern Sakhalin slope, separated elongate drifts on the slope of the North Okhotsk margin, mounded confined drift between exposed rotated basement blocks, as well as elongate mounded drifts north of Sakhalin Island.

Downslope processes are also important on the northern Sakhalin margin. They include: (1) basinward shifts of the depocenters during sea-level lowstands, and (2) repeated mass wasting that has probably changed the original convex cross-section of the NIA on the northern Sakhalin slope to a concave form, excavating large volumes of sediments which are deposited as slumps and debris flows in the western Derugin Basin (Fig. 12). These mass wasting events are possibly triggered by earthquakes, or over-steepening and/or pore-water over-pressuring as a result of rapid sedimentation. Triggering by destabilization of gas hydrates during sea-level lowstands may also have been important.

During glacial periods, sediments discharged by the Amur River are laid down partly as lowstand deltaic wedges north of Sakhalin Bay and partly as giant confined drift bodies in the Staretsky Trough and on the North Okhotsk margin. During interglacial times, the bulk of the Amur sediments is deposited as drifts or as a 'fan' on the southern Sakhalin margin outside our study area.

Acknowledgements

We gratefully acknowledge the unfailing help of the captains, officers, crew and in particular the scientific parties of the R/V *Professor Gagarinsky* during the four Sea of Okhotsk cruises reported here (cruises 16, 22, 26 and 32). Our thanks are also due to Dr. Lionel Carter, Dr. Antoon Kuijpers and Dr. David J.W. Piper for their valuable constructive reviews, which led to a substantial improvement of the manuscript. This work was carried out within the framework of the German–Russian cooperative KOMEX project funded by the German Federal Ministry of Education and Research (Projects 03G0535D and 03G0068B) and by the Russian Ministry of Industry and Science. We are grateful for their financial support, which made this study possible.

References

Alfultis, M.A., Martin, S., 1987. Satellite passive microwave studies of the Sea of Okhotsk ice cover and its relation to oceanic processes, 1978-1982. J. Geophys. Res. C 92, 13013–13028.

Astakhov, A., Botsul, A., Biebow, N., Derkachev, A., Fessler, S., Gorbarenko, S., Kaiser, A., Nikolayeva, N., Tiedemann, R., Werner, R., 2000. Paleoceanography and sedimentology. In: Biebow, N., Lüdmann, T., Karp, B., Kulinich, R. (Eds.), KOMEX Cruise Reports: KOMEX V and VI, RV *Professor Gagarinsky* Cruise 26, MV *Marshal Gelovany* Cruise 1. GEOMAR Report 88, 189–209.

Barnes, P.M., Lewis, K.B., 1991. Sheet slides and rotational failures on a convergent margin: the Kidnappers Slide, New Zealand. Sedimentology 38, 205–221.

Biebow, N., Hütten, E. (Eds.), 1999. KOMEX Cruise Reports: KOMEX I and II, RV *Professor Gagarinsky* Cruise 22, RV *Akademik M.A. Lavrentyev* Cruise 28. GEOMAR Report 82, 188+89 pp.

Biebow, N., Tiedemann, R., Gorbarenko, S., Nürnberg, D., Kaiser, A., Derkachev, A., Matul, A., Werner, R., 2000. Stratigrapgy and general patterns of sediment deposition in the Sea of Okhotsk - an overview. In: Programs and Abstracts, 3rd Workshop on Russian-German Cooperation in the Okhotsk Sea-Kurile Island Arc System, Moscow, April 17–20, 2000, pp. 17–18.

Bugge, T., Befring, S., Belderson, R.H., Eidvin, T., Jansen, E., Kenyon, N.H., Holtedahl, H., Sejrup, H.P., 1987. A giant three-stage submarine slide off Norway. Geo-Mar. Lett. 7, 191–198.

Carter, L., McCave, I.N., 1994. Development of sediment drifts approaching an active margin under the SW Pacific Deep Western Boundary Undercurrent. Paleoceanography 9, 1061–1085.

Chapman, M.E., Solomon, S.C., 1976. North American-Eurasian plate boundary in northeast Asia. J. Geophys. Res. 81, 921–930.

Evans, D., King, E.L., Kenyon, N.H., Brett, C., Wallis, D.,

1996. Evidence for long term instability in the Storegga Slide region off western Norway. Mar. Geol. 130, 281–292.
Elverhøi, A., Norem, H., Andersen, E.S., Dowdeswell, J.A., Fossen, I., Haflidason, H., Kenyon, N.H., Laberg, J.S., King, E.L., Sejrup, H.P., Solheim, A., Vorren, T., 1997. On the origin and flow behavior of submarine slides on deep-sea fans along the Norwegian-Barents Sea continental margin. Geo-Mar. Lett. 17, 119–125.
Faugères, J.-C., Mézerais, M.-L., Stow, D.A.V., 1993a. Contourite drift types and their distribution in the North and South Atlantic Ocean basins. Sediment. Geol. 82, 189–203.
Faugères, J.-C., Mézerais, M.-L., Stow, D.A.V., 1993b. Bottom-current-controlled sedimentation: a synthesis of the contourite problem. Sediment. Geol. 82, 287–297.
Faugères, J.-C., Stow, D.A.V., Imbert, P., Viana, A., 1999. Seismic features diagnostic of contourite drifts. Mar. Geol. 162, 1–38.
Favorite, F.A., Dodimead, A.J., Nasu, K., 1976. Oceanography of the Subarctic Pacific Region, 1960-1976. Int. N. Pac. Fish. Commun. 33, 187 pp.
Freeland, H.J., Bychkov, A.S., Whitney, F., Taylor, C., Wong, C.S., Yurasov, G.I., 1998. WOCE section P1W in the Sea of Okhotsk - 1. Oceanographic data description. J. Geophys. Res. C 103, 15613–15623.
Frenzel, B., Pesci, M., Velichko, A.A., 1992. Atlas of Paleoclimates and Paleoenvironments of the Northern Hemisphere - Late Pleistocene-Holocene. Gustav Fischer, Budapest.
Fulthorpe, C.S., Carter, M.C., 1991. Continental-shelf progradation by sediment-drift accretion. Geol. Soc. Am. Bull. 103, 300–309.
Gladyshev, S.V., 1995. Fronts in the Kurile Islands region. Oceanography 34, 452–459.
Gladyshev, S., Martin, S., Riser, S., Figurkin, A., 2000. Dense water production on the northern Okhotsk shelves: comparison of ship-based spring-summer observations for 1996 and 1997 with satellite observations. J. Geophys. Res. C 105, 26281–26299.
Gnibidenko, H.S., Khvedchuk, I.I., 1982. The tectonics of the Okhotsk Sea. Mar. Geol. 50, 155–198.
Gorbarenko, S.A., 1991. The stratigraphy of the upper Quaternary sediments in the central part of the Sea of Okhotsk and its paleoceanology according to data obtained by the $\delta^{18}O$ and other methods. Oceanology 31, 761–766.
Gorbarenko, S.A., Kovalyukh, N.N., Odinokova, L.Yu., Rybakov, V.F., Tokarchuk, T.N., Shapovalov, V.V., 1990. Upper Quaternary sediments of the Sea of Okhotsk and the reconstruction of paleoceanologic conditions. Geol. Pac. Ocean 6, 309–330.
Gorbarenko, S., Nürnberg, D., Leskov, V., Tiedemann, R., Kaiser, A., Biebow, N., Artemova, A., 2000. Suborbital climate changes in the Okhotsk Sea during the last 75 thousand years: evidence by ice-rafted debris and metal geochemistry. In: Programs and Abstracts, 3rd Workshop on Russian-German Cooperation in the Okhotsk Sea-Kurile Island Arc System, Moscow, April 17–20, 2000, pp. 27–28.
Haq, B.U., 1991. Sequence stratigraphy, sea-level change, and significance for the deep-sea. Int. Assoc. Sedimentol. Spec. Publ. 12, 3–39.
Haq, B.U., 1998. Natural gas hydrates: searching for the long-term climatic and slope-stability records. In: Henriet, J.-P., Mienert, J. (Eds.), Gas Hydrates: Relevance to World Margin Stability and Climate Change. Geol. Soc. Lond. Spec. Publ. 137, 303–318.
Harris, P.T., Brancolini, G., Armand, L., Busetti, M., Beaman, R.J., Giorgetti, G., Presti, M., Trincardi, F., 2001. Continental shelf drift deposit indicates non-steady state Antarctic bottom water production in the Holocene. Mar. Geol. 179, 1–8.
Hollister, C.D., Heezen, B.C., 1972. Geological effects of ocean bottom currents: western North Atlantic. In: Gordon, A.L. (Ed.), Studies in Physical Oceanography, vol. 2. Gordon and Breach, New York, pp. 37–66.
Hopkins, D.M., 1972. The paleogeography and climatic history of Beringia during late Cenozoic time. Internord 12, 121–150.
Kaiser, A., Nürnberg, D., Tiedemann, R., 2002. Glacial history in NE Siberia - Implications from IRD and stable oxygen isotope records. Program and Abstracts, 'Climate Drivers of the North', Kiel, May 8–11, 2002. Terra Nostra, 2002/3, 53.
Kayen, R.E., Lee, H.J., 1993. Slope instability in regions of seafloor gas hydrate: Beaufort Sea continental slope. In: Swab, W.C., Lee, H.J., Twichell, D.C. (Eds.), Submarine Slides: Selected Studies in the U.S. Exclusive Economic Zone. U.S. Geol. Surv. Bull. B2 1502, 97–103.
Keigwin, L.D., 1998. Glacial-age hydrography of the far northwest Pacific. Paleoceanography 13, 323–339.
Kitani, K., 1973. An oceanographic study of the Sea of Okhotsk particularly in regard to cold waters. Bull. Far Seas Fish. Res. Lab. 9, 45–77.
Kitani, K., Shimazaki, K., 1971. On the hydrography of the northern part of the Sea of Okhotsk in summer. Bull. Fac. Fish. Hokkaido Univ. 12, 231–242.
Kononov, V.E., Sergeev, K.F., Argentov, V.V., Bikkenina, C.K., Zhigulev, V.V., Zhiltsov, E.G., 1998. Possibilities of the seismic refraction method for hydrocarbon potential investigations on the northeastern shelf of Sakhalin Island (in Russian). Tikhookeanskaya Geologiy 17, 27–38.
Kowalik, Z., Polyakov, I., 1998. Tides in the Sea of Okhotsk. J. Phys. Oceanogr. 28, 1389–1409.
Kowalik, Z., Polyakov, I., 1999. Diurnal tides over Kashevarov Bank, Okhotsk Sea. J. Geophys. Res. 104, 5361–5380.
Kuipers, A., Nielsen, T., Akhmetzhanov, A., de Haas, H., Kenyon, N.H., van Weering, T.C.E., 2000. Late Quaternary slope instability on the Faeroe margin: mass flow features and timing of events. Geo-Mar. Lett. (on-line) 10.1007/s003670000053.
Kwiek, P.B., Ravelo, A.C., 1999. Pacific Ocean intermediate and deep water circulation during the Pliocene. Paleogeogr. Paleoclimatol. Paleoecol. 154, 191–217.
Laberg, J.S., Vorren, T.O., Mienert, J., Bryn, P., Lien, R., 2002. The Trænadjupet Slide: a large slope failure affecting the continental margin of Norway 4,000 years ago. Geo-Mar. Lett. 22, 19–24.

Leonev, A.K., 1960. The Sea of Okhotsk. NTIS AD 639 585. Natl. Tech. Inform. Services, Springfield, 95 pp.

Leskov, V., Kaiser, A., Gorbarenko, S., Tiedemann, R., Biebow, N., Nürnberg, D., Matul, A., 2000. Spatial and temporal variability of sea ice cover in the Okhotsk Sea during the last 75 ka: evidence from IRD time slice reconstructions. In: Programs and Abstracts, 3rd Workshop on Russian-German Cooperation in the Okhotsk Sea-Kurile Island Arc System, Moscow, April 17–20, 2000, pp. 39–40.

Lüdmann, T., Wong, H.K., 2003. Seismic characteristics of areas of gas venting and gas hydrate occurrence in the northwestern Sea of Okhotsk. Mar. Geol. doi:10.1016/S0025-3227(03)00224-X, in press.

Maslin, M.A., Haug, G.H., Sarnthein, M., Tiedemann, R., 1996. The progressive intensification of northern hemisphere glaciation as seen from the North Pacific. Geol. Rundsch. 85, 452–465.

Masson, D.G., Howe, J.A., Stoker, M.S., 2002. Bottom-current sediment waves, sediment drifts and contourites in the northern Rockall Trough. Mar. Geol. 192, 215–237.

Mienert, J., Posewang, J., 1999. Evidence of shallow- and deep-water gas hydrate destabilizations in North Atlantic polar continental margin sediments. Geo-Mar. Lett. 19, 143–149.

Mizuta, G., Fukamachi, Y., Ohshima, K.I., Wakatsuchi, M., 2001. Southward current off the east coast of Sakhalin in the Sea of Okhotsk observed from 1998 to 2000. 6th Int. Symposium on Okhotsk Sea and Sea Ice, Mombetsu, Hokkaido, 4–8 Feb., 2001. Abstr. Vol., pp. 198–205.

Morley, J.J., Heusser, L.E., Shackleton, N.J., 1991. Late Pleistocene/Holocene radiolarian and pollen records from sediments in the Sea of Okhotsk. Paleoceanography 6, 121–131.

Nelson, C.H., Baraza, J., Maldonaldo, A., 1993. Mediterranean undercurrent sandy contourites, Gulf of Cadiz, Spain. Sediment. Geol. 82, 103–131.

Nürnberg, D., Baranov, B.V., Karp, B.Ya., 1997. Cruise Report: RV *Akademik M.A. Lavrentyev* Cruise 27 (GREGORY Cruise). GEOMAR Report 60, 69+74 pp.

Nürnberg, D., Kaiser, A., Tiedemann, R., Biebow, N., 2002. Paleoceanographic studies in the Sea of Okhotsk - Implications for the glaciation history of NE Siberia. Program and Abstracts, 'Climate Drivers of the North', Kiel, May 8–11, 2002. Terra Nostra, 2002/3, 81–82.

Nürnberg, D., Tiedemann, R., Kaiser, A., Kozdon, R., Lembke, L., Biebow, N., Roehl, U., 2002. Orbital to suborbital paleoceanographic and paleoclimatic changes in the Sea of Okhotsk. Program and Abstracts, 'Climate Drivers of the North', Kiel, May 8–11, 2002. Terra Nostra, 2002/3, 83.

Polyakov, I., Martin, S., 2000. Interaction of the diurnal tides with the Kashevarov Bank polynya. J. Geophys. Res. C 106, 3281–3294.

Posamentier, H.W., Jervey, M.T., Vail, P.R., 1988. Eustatic control on clastic deposition: I. Conceptual framework. In: Wilgus, C.K., Hastings, B.S., Kendall, C.G.St.C., Posamentier, H.W., Ross, C.A., van Wagoner, J.C. (Eds.), Sea-level Changes - An Integrated Approach. SEPM Spec. Publ. 42, 110–124.

Rea, D.K., Basov, I.A., Janecek, T.R., Palmer-Julson, A., et al., 1993. Proc. ODP Init. Repts. 145, 1040 pp.

Rea, D.K., Schrader, H., 1985. Late Pliocene onset of glaciation: Ice-rafting and diatom stratigraphy of North Pacific DSDP cores. Paleogeogr. Paleoclimatol. Paleoecol. 49, 313–325.

Reed, D.L., Meyer, A.W., Silver, E.A., Prasetyo, H., 1987. Contourite sedimentation in an intraoceanic forearc system: eastern Sunda Arc, Indonesia. Mar. Geol. 76, 223–242.

Rodnikov, A.G., Tuezov, I.K., Kharakhinov, V.V. (Eds.), 1996. Structure and Dynamics of the Lithosphere and Asthenosphere of the Okhotsk Sea Region. National Physical Committee, Russian Acad. Sci., Moscow, 335 pp. (in Russian).

Rogachev, K.A., Carmack, E.C., Salomatin, A.S., 2000. Strong tidal mixing and ventilation of cold intermediate water at Kashevarov Bank, Sea of Okhotsk. J. Oceanogr. 56, 439–447.

Rothwell, R.G., Thomson, J., Kähler, G., 1998. Low-sea-level emplacement of a very large Late Pleistocene 'megaturbidite' in the western Mediterranean Sea. Nature 329, 377–380.

Sancetta, C., 1983. Effect of Pleistocene glaciation upon oceanographic characteristics of the North Pacific Ocean and Bering Sea. Deep-Sea Res. 30 (8A), 851–869.

Savostin, L., Zonenshain, L., Baranov, B., 1983. Geology and plate tectonics of the Sea of Okhotsk. In: Hilde, T.W.C., Uyeda, S. (Eds.), Geodynamics of the Western Pacific-Indonesian Region, Geodynamics Ser. 11. AGU, Washington, DC, pp. 189–221.

Seno, T., Sakurai, T., 1996. Can the Okhotsk plate be discriminated from the North American plate? J. Geophys. Res. B 101, 11305–11315.

Shevchenko, G.V., Putov, V.F., 1999. On wind and tide induced sea-ice drift on the northeastern shelf of Sakhalin Island (analysis of radar data). In: Lobanov, V.B., Nagata, Y., Riser, S.C. (Eds.), Proc. Second PICES Workshop on the Okhotsk Sea and Adjacent Areas. PICES Scientific Report 12, pp. 11–18.

Shiga, K., Koizumi, I., 2000. Latest Quaternary oceanographic changes in the Okhotsk Sea based on diatom records. Mar. Micropaleontol. 38, 91–117.

Stoker, M.S., 1998. Sediment drift development on the Rockall continental margin off NW Britain. In: Stoker, M.S., Evans, D., Cramp, A. (Eds.), Geological Processes on Continental Margins: Sedimentation, Mass-Wasting and Stability, Geol. Soc. Lond. 129, 229–254.

Talley, L.D., 1991. An Okhotsk Sea water anomaly: Implications for ventilations in the North Pacific. Deep-Sea Res. 1, 171–190.

Talley, L.D., Nagata, Y., 1995. The Okhotsk Sea and Oyashio region. 2. North Pacific Marine Science Organisation (PICES), PICES Scientific Rept. No. 2, Rept. of Working Group 1, 227 pp.

Tiedemann, R., Nürnberg, D., Kozdon, R., Lembke, L., Kaiser, A., Kokfelt, U., 2002. Holocene multidecadal tocentennial climate variability in the Sea of Okhotsk. Program and

Abstracts, 'Climate Drivers of the North', Kiel, May 8–11, 2002. Terra Nostra, 2002/3, 110–111.

Vail, P.R., Audmard, F., Bowman, S.A., Eisner, P.N., Perez Cruz, C., 1991. The stratigraphic signatures of tectonics, eustacy, and sedimentology - an overview. In: Einsele, G., Ricken, W., Seilacher, A. (Eds.), Cycles and Events in Stratigraphy. Springer, Berlin, pp. 617–659.

van Weering, T.C.E., Nielsen, T., Kenyon, N.H., Akentieva, K., Kuipers, A.H., 1998. Sediments and sedimentation at the NE Faeroe continental margin: contourites and large-scale sliding. Mar. Geol. 152, 159–176.

Vogt, P.R., Gardner, J., Crane, K., 1999. The Norwegian-Barents-Svalbard (NBS) continental margin: Introducing a natural laboratory of mass wasting, hydrates, and ascent of sediment, pore water, and methane. Geo-Mar. Lett. 19, 2–21.

Wong, C.S., Matear, R.J., Freeland, H.J., Whitney, F.A., Bychkov, A.S., 1998. WOCE line P1W in the Sea of Okhotsk 2. CFCs and the formation rate of intermediate water. J. Geophys. Res. C 103, 15625–15642.

Worrall, D.M., Kruglyak, V., Kunst, F., Kuznetsov, V., 1996. Tertiary tectonics of the Sea of Okhotsk, Russia: far-field effects of the India-Eurasia collision. Tectonics 15, 813–826.

Yang, J., Honjo, S., 1996. Modelling the near freezing dichothermal layer in the Sea of Okhotsk and its interannual variations. J. Geophys. Res. C 101, 16421–16433.

Zhuravlev, A.V., 1984. Comparison between the Derugin and Tinro basins of the Okhotsk Sea (in Russian). Geol. Pac. 4, 21–27.